

Scalable Generation and Characterization of a Four-Photon Twelve-Qubit Hyperentangled State

Kun Du^a and Cong-Feng Qiao^{a,b*}

^aDepartment of Physics, Graduate University of Chinese Academy of Sciences,
Beijing 100049, China

^bTheoretical Physics Center for Science Facilities (TPCSF),
CAS, Beijing 100049, China

An experimentally feasible scheme for generating a 12-qubit hyperentangled state via four photons, entangled in polarization, frequency and spatial mode, is proposed. We study the nature of quantum non-locality of this hyperentangled state by evaluating its violation degree to a Bell-type inequality, and find that the result agrees well with quantum mechanics prediction while extremely contradicts to the local realism constraint.

Keywords: hyperentanglement; Bell inequality; non-locality; Qubit

1 Introduction

Qubit is the basic information unit of quantum computer. Hence, the generation of multi-qubit entangled states keeps as an essential task in quantum information processing and transmission [1]. Quantum entanglement, especially multipartite entanglement, has many important applications, such as measurement-based quantum computing [2], secure superdense coding [3], teleportation [4], entanglement purification [5] and quantum cryptography [6]. However, the experimental realization of multipartite entanglement is still a significant

*Corresponding author. Email: qiaocf@gucas.ac.cn

challenge. People realized that the manipulation of more than six photons without quantum storage turns out to be an insurmountable obstacle with present technology [7]. However, the hyperentanglement(HE), which in practice remains in many physical systems, tends to be an effective and practical way [8, 9, 10] to manipulate more qubits effectively, namely making the quanta, e.g. photons, to be entangled simultaneously in multiple degrees of freedom (DOFs). Furthermore, HE states are much less affected by decoherence and are particular important in the realization of even more challenging objectives in comparison with the normal entangled states.

Recently, two-photon four-qubit states [11, 12, 13] and two-photon six-qubit states [14, 15] were experimentally realized, and found to offer significant enhancement of the channel capacity in superdense coding [16, 17], to construct efficiently the fourqubit two-photon cluster states [18], and to realize successfully the basic quantum computation algorithms in the one-way model [11, 19]. More recently, Jian-Wei Pan *et al.* generated in experiment the hyperentangled ten-qubit photonic Schrödinger cat state by exploiting polarization and momentum of five photons [7]. In this article, we propose an experimentally practical scheme for generating a four-photon twelve-qubit hyperentangled state entangled in three DOFs, i.e. in polarization, frequency and spatial mode.

Nonlocality is a unique feature of Quantum Mechanics(QM) differing from the local realism(LR) theory. People found that the HE states can enhance the violation of LR [20]. We find in this work that the twelve-qubit hyperentangled state exhibits extremely large violation of the LR constraint by evaluating a Bell-type inequality. Furthermore, we show generally that the more the entangled degrees of freedom are, the stronger the violation of Bell-type inequality will be

The structure of the paper goes as follows: in section 2, an experimentally feasible scheme for the production and measurement of a four-photon twelve-qubit hyperentangled state is proposed. In section 3, we discuss the quantum characteristics of the hyperentangled state(mathematic details are presented in Appendix). A brief summary and concluding remarks are given in section 4.

2 Preparation scheme for hyperentangled state

The hyperentangled state to be generated in our scheme takes the following form up to a normalization constant:

$$|\psi\rangle = (|HHHH\rangle + |VVVV\rangle) \otimes (|\omega_1\omega_2\omega_1\omega_2\rangle + |\omega_2\omega_1\omega_2\omega_1\rangle) \otimes (|a'_1b'_1c'_1d'_1\rangle + |a'_2b'_2c'_2d'_2\rangle), \quad (1)$$

where H and V denote horizontal and vertical polarization, ω_1 and ω_2 signify different frequency and $a'_1, b'_1, c'_1, d'_1, a'_2, b'_2, c'_2, d'_2$ label eight different spatial modes. The state (1) shows maximal entanglement among all photons' degrees of freedom in polarization, frequency and spatial modes. This state is a Schrödinger cat state, and can also be called as Greenberger-Horne-Zeilinger state [21], which possesses peculiar interest in quantum information science.

To generate the state, the first step is to produce two pairs of two-dimensional hyperentangled photons, as shown in Figure 1a, via two adjacent thin type-II barium borate (BBO) crystals [22]. The photon pairs can be generated by spontaneous parametric down-conversion (SPDC) [23] and entangled in polarization and frequency DOFs [24]. If pump photon downconvert in first (second) crystal, the frequency of the signal photon will be ω_1 (ω_2), and hence the Idler photon takes the opposite. In case a pump pulse coming from left (right) threads the first (second) set of crystal, a pair of photons will be produced in the spatial modes a_1 and b_1 (c_1 and d_1). Similarly, a pair of hyperentangled photons can be produced in spatial modes a_2 and b_2 (c_2 and d_2) [5] while the pump pulse is reflected by the mirror behind the crystal and then threads the crystal second time. Since one can simply adjust the relative phase between the first and second possibilities, two pairs of photons in the following form are readily obtained:

$$(|HH\rangle + |VV\rangle) \otimes (|\omega_1\omega_2\rangle + |\omega_2\omega_1\rangle) \otimes (|a_1b_1\rangle + |a_2b_2\rangle), \quad (2)$$

$$(|HH\rangle + |VV\rangle) \otimes (|\omega_1\omega_2\rangle + |\omega_2\omega_1\rangle) \otimes (|c_1d_1\rangle + |c_2d_2\rangle). \quad (3)$$

Next, we employ the two non-entangled photons a and c in above two pairs to make all photons entangled in polarization and spatial mode. Obviously, photons a and c are in the state of the form

$$[(|H\rangle + |V\rangle) \otimes (|a_1\rangle + |a_2\rangle)] \otimes [(|H\rangle + |V\rangle) \otimes (|c_1\rangle + |c_2\rangle)]. \quad (4)$$

As shown in Figure 1b, photons in paths a_1 and c_1 (a_2 and c_2) frontally enter Polarizing Beam Splitters (PBSs). Since the PBS transmits H and reflects V polarization photons, we can then come to a conclusion that if the two photons pass through paths a'_1 and c'_1 (a'_2 and c'_2) simultaneously, it implies that both of the photons are H or V polarized. Afterwards, photons in modes a'_1 , c'_1 , a'_2 and c'_2 are led to a cross-kerr nonlinear medium [25, 26] as shown in Figure 2, which brings forth an adjustable phase shift to the coherent state $|\alpha\rangle$ through cross-phase modulation (XPM), e.g. 3θ , -2θ , 2θ and $-\theta$ for four modes, respectively. Then we perform the X homodyne detection on the coherent state $|\alpha\rangle$ [27]. In case the measured phase shift is θ , the state will be kept. In the end, the reserved states of photons a and c can only come out from a'_1 and c'_1 or a'_2 and c'_2 . That means the states of photons a and c are in the following entangled form:

$$(|HH\rangle + |VV\rangle) \otimes (|a'_1c'_1\rangle + |a'_2c'_2\rangle). \quad (5)$$

Similarly, we can use another pair of non-entangled photons b and d to make all photons entangled in spacial mode and frequency. As mentioned in above, the initial photons b and d are in the state:

$$[(|\omega_1\rangle + |\omega_2\rangle) \otimes (|b_1\rangle + |b_2\rangle)] \otimes [(|\omega_1\rangle + |\omega_2\rangle) \otimes (|d_1\rangle + |d_2\rangle)]. \quad (6)$$

Connecting paths b_1 , b_2 , d_1 and d_2 with four optical demultiplexers (OD) respectively, which are part of Wavelength Division Multiplex (WDM) [28], we then separate each mode into two in terms of frequency as shown in Figure 1c. The modes b_{11} , b_{21} , d_{11} and d_{21} correspond to frequency ω_1 , while the modes b_{12} , b_{22} , d_{12} and d_{22} correspond to ω_2 . Taking the same procedure as for modes a and c , we lead these eight paths to another cross-kerr nonlinear medium, as shown Figure 3, which induces the coherent state $|\alpha'\rangle$ phase shifts of 2θ , 4θ , $-\theta$, -3θ , 3θ , 5θ , -2θ and -4θ , respectively. After performing the X homodyne detection on $|\alpha'\rangle$, we retain those states with phase shift θ . Then, photons b and d should pass through in one pair of the four paths, i.e. b_{11} - d_{11} , b_{12} - d_{12} , b_{21} - d_{21} , and b_{22} - d_{22} . At last, let those two paths originated from the same path via OD link to an optical multiplexer(OM), which is other part of WDM and can merge them into one path. For instance, paths b_{11} - b_{12} , which both come from b_1 by OD, are merged into b'_1 after passing through OM. After taking above

procedures, photons b and d then lie in the state of the following entangled form:

$$(|\omega_1\omega_1\rangle + |\omega_2\omega_2\rangle) \otimes (|b'_1d'_1\rangle + |b'_2d'_2\rangle). \quad (7)$$

In all, from (2), (3), (5) and (7), we find that a four-photon 12-qubit hyperentangled state (1) is created. Unfortunately, the setups shown in Figures 2 and 3 are generally impossible to change the sign of the phase shift in single nonlinear medium. The signs of the phase shifts must be identical, since they are all proportional to the nonlinear susceptibility χ^3 [29]. To circumvent this difficulty, at least one can use either the cross-kerr with two materials of opposite nonlinearities instead of the single material, or use double XPM method [30] without minus phase as shown in Figures 4 and 5. In Figure 4, we use a 50:50 beam splitter (BS) to divide the coherent state into two beams $|\alpha\rangle$ $|\alpha\rangle$, and then they are coupled to the photonic modes a'_1 and a'_2 , c'_1 and c'_2 through the XPM respectively. Correspondingly, the phase shifts induced by the couplings are θ and 2θ in both beams. Afterwards, the two coherent states after the interaction are compared with a 50-50 BS. Project the $|n\rangle\langle n|$ onto the upper beam, in case $n = 0$, the state (5) is obtained. Analogously, we can obtain the state (7) with the same procedure as presented in Figure 5.

A setup for measuring the hyperentanglement in polarization, frequency and spatial mode simultaneously and independently is schematically shown in Figure 6. Place eight of these setups in all eight output paths, the qubits in spatial mode can then be determined. Of each spatial mode, the optical demultiplexer splits it into two paths according to frequency, which means one therefore obtains the qubits in frequency. Subsequently, at both of these two paths the conventional polarization analysis [31] is implemented, by which the qubits in polarization are read out.

3 Quantum characteristics of the hyperentangled state

To characterize the hyperentangled state (1), we evaluate the Bell-type inequality violation of it. Note that the 12-qubit state (1) is the eigenstate of 2^{12} stabilizing operators with unit eigenvalue [32, 33]. i.e.,

$$S_i|\psi\rangle = |\psi\rangle, i = 1, 2, \dots, 2^{12}, \quad (8)$$

where

$$S_i = \bigotimes_{k=1}^3 O_j^{(k)} \quad (9)$$

describe perfect correlations in the state. Here, $O_j^{(k)} \in \{I, \pm X_j^{(k)}, \pm Y_j^{(k)}, \pm Z_j^{(k)}\}$ represent the observables for each photon. I and $X_j^{(k)}, Y_j^{(k)}, Z_j^{(k)}$ denote the identity and Pauli matrices, with subscript $j = 1, 2, 3, 4$ signifying photons a, b, c and d , and superscript $k = 1, 2, 3$ signifying the three DOF. The operators X, Y , and Z satisfy relationship $ZX = -XZ = iY$.

According to Ref.[34] the Bell operator can be expressed as

$$B = \sum_i^{2^{12}} S_i . \quad (10)$$

The local hidden variable theory(LHVT) sets the upper bound for the expectation value of B , and hence satisfies the following inequality [35]

$$\langle B \rangle \leq \max_{LHVT} |\langle B \rangle| . \quad (11)$$

We notice that among all 4096 S_i , there are 1854 of them with negative signs in front as shown in the Appendix, like

$$-Y_1^{(1)} Y_2^{(1)} X_3^{(1)} X_4^{(1)} |\psi\rangle = |\psi\rangle .$$

In LHVT, the observables are elements of reality, that means their values are precisely defined, i.e. either +1 or -1 [36]. Therefore, the upper bound of the expectation value of B in (10) is $2^{12} - 2 \times 1854 = 388$. On the other hand, in quantum mechanics, the expectation value of B is $2^{12} = 4096$. Obviously, the QM result greatly violates the inequality (11), the bound set by the LHVT.

Following, we compare the degrees of violation of different GHZ-type states with same amount of qubits but different numbers of photons. According to the Appendix, one may conclude that the more the entangled degrees of freedom are, the stronger the violation of Bell-type inequality will be. To give a concrete example, in Table 1 we compare the violation degrees to the Bell-type inequality of three different 12-qubit entangled states, that is (1),

$$|\psi'\rangle = (|HHHHHH\rangle + |VVVVVV\rangle) \bigotimes (|\omega_1\omega_2\omega_1\omega_2\omega_1\omega_2\rangle + |\omega_2\omega_1\omega_2\omega_1\omega_2\omega_1\rangle) , \quad (12)$$

and

$$|\psi''\rangle = (|HHHHHHHHHHHH\rangle + |VVVVVVVVVVVV\rangle). \quad (13)$$

The results in the Table indicate that the state (1) entangled in three DOFs violates the Bell inequality (11) most, the state (12) entangled in two DOFs goes next, and the state (13) entangled in only one DOF violates the Bell inequality least.

4 Conclusions

In summary, in this work we propose a novel scheme for the generation of simultaneous entanglement of four photons in three independent DOFs, i.e., a 12-qubit hyperentangled state, by virtue of the linear optical instrument and cross-Kerr nonlinearity. We show that the proposed scheme is within the reach of nowadays technology. Theoretically, our method can be simply expanded to the production of hyperentangled state with more photons, although practically the difficulties in the manipulation of six or more photons make the expansion non-realistic. To check the nonlocality nature of this 12-qubit hyperentangled state, we evaluate its violation degree to a Bell-type inequality. The result agrees well with the QM prediction while extremely contradicts to the LR constraint, which indicates that the genuine multiparticle hyperentangled state possesses certain superiority in comparison with the normal entangled state in the verification of QM nonlocality, quantum computation, and quantum information processing.

Acknowledgments

This work was supported in part by the National Natural Science Foundation of China(NSFC), by the CAS Key Projects KJCX2-yw-N29 and H92A0200S2. We thank Junli Li, Hongbo Xu and Chao Niu for useful discussions.

References

- [1] Nielsen, M.A. and Chuang, I.L., *Quantum Computation and Quantum Information* (Cambridge University Press, Cambridge, England, **2000**).
- [2] Raussendorf, R.; Briegel, H. J., *Phys. Rev. Lett.* **2001**, 86, 5188-5191.
- [3] Wang, C.; Deng, F.G.; Li, Y.S.; Liu, X.S. and Long, G.L., *Phys. Rev. A* **2005**, 71, 044305.
- [4] Bennett, C.H.; Brassard, C.; Crépeau, C.; Jozsa, R.; Peres, A.; Wootters, W.K., *Phys. Rev. Lett.* **1993**, 70, 1895.
- [5] Simon, C.; Pan, J.W., *Phys. Rev. Lett.* **2002**, 89, 257901.
- [6] Bruss, D.; Macchiavello, C., *Phys. Rev. Lett.* **2002**, 88, 127901.
- [7] Gao, W.B.; Lu, C.Y.; Yao, X.C.; Xu, P.; Gühne, O.; Goebel, A.; Chen, Y.A.; Peng, C.Z.; Chen, Z.B.; Pan, J.W., *Nature Physics* **2010**, 6, 331.
- [8] Kwiat, P. G., *J. Mod. Opt.* **1997**, 44, 2173.
- [9] Kwiat, P.G.; Waks, E.; White, A.G.; Appelbaum, I.; Eberhard, P.H., *Phys. Rev. A* **1999**, 60, R773.
- [10] Barbieri, M.; Cinelli, C.; Mataloni, P.; De-Martini, F., *Phys. Rev. A* **2005**, 72, 052110.
- [11] Chen, K.; Li, C.M.; Zhang, Q.; Chen, Y.A.; Goebel, A.; Chen, S.; Mair, A.; Pan, J.W., *Phys. Rev. Lett.* **2007**, 99, 120503.
- [12] Yang, T.; Zhang, Q.; Zhang, J.; Yin, J.; Zhao, Z.; Żukowski, M.; Chen, Z.B.; Pan, J.W., *Phys. Rev. Lett.* **2005**, 95, 240406.
- [13] Chen, Z.B.; Pan, J.W.; Zhang, Y.D.; Časlav Brukner; Zeilinger, A., *Phys. Rev. Lett.* **2003**, 90, 160408.
- [14] Vallone, G.; Ceccarelli, R.; Martini, F.D.; Mataloni, P., *Phys. Rev. A* **2009**, 79, R030301.

- [15] Barreiro, J.T.; Langford, N.K.; Peters, N.A.; Kwiat, P.G., *Phys. Rev. Lett.* **2005**, 95, 260501.
- [16] Schuck, C.; Huber, G.; Kurtsiefer, C. and Weinfurter, H., *Phys. Rev. Lett.* **2006**, 96, 190501.
- [17] Barreiro, J. T.; Wei, T. C. and Kwiat, P. G., *Nature Phys.* **2008**, 4, 282.
- [18] Vallone, G.; Pomarico, E.; Martini, F. De and Mataloni, P., *Phys. Rev. Lett.* **2008**, 100, 160502.
- [19] Briegel, H. J. and Raussendorf, R., *Phys. Rev. Lett.* **2001**, 86, 910.
- [20] Barbieri, M.; Martini, F. D.; Mataloni, P.; Vallone, G. and Cabello, A., *Phys. Rev. Lett.* **2006**, 97, 140407.
- [21] Greenberger, D.M.; Horne, M.; Shimony, A.; Zeilinger, A., *Am. J. Phys.* **1990**, 58, 1131.
- [22] Kwiat, P.G.; Mattle, K.; Weinfurter, H.; Zeilinger, A., *Phys. Rev. Lett.* **1995**, 75, 4337.
- [23] Walborn, S.P.; De-Oliveira, A.N.; Thebaldi, R.S.; Monken, C.H., *Phys. Rev. A* **2004**, 69, 023811.
- [24] Yabushita, A.; Kobayashi, T., *Phys. Rev. A* **2004**, 69, 013806.
- [25] Sheng, Y.B.; Deng, F.G.; Zhou, H.Y., *Phys. Rev. A* **2008**, 77, 042308.
- [26] Sheng, Y.B.; Deng, F.G.; Long, G.L., *Phys. Rev. A* **2010**, 82, 032318.
- [27] Nemoto, K.; Munro, W.J., *Phys. Rev. Lett.* **2004**, 93, 250502.
- [28] Sheng, Y.B.; Deng, F.G., *Phys. Rev. A* **2010**, 81, 032307.
- [29] Kok, P., *Phys. Rev. A* **2008**, 77, 013808.
- [30] He, B.; Ren, Y.H.; Bergou, J.A., *Phys. Rev. A* **2009**, 79, 052323.

- [31] Vallone, G.; Pomarico, E.; Mataloni, P.; De-Martini, F.; Berardi, V., *Phys. Rev. Lett.* **2007**, 98, 180502.
- [32] Cabello, A.; Rodriguez, D.; Villanueva, I., *Phys. Rev. Lett.* **2008**, 101, 120402.
- [33] Géza-Tóth; Gühne, O., *Phys. Rev. A* **2005**, 72, 022340.
- [34] Gühne, O.; Géza-Tóth; Hyllus, P.; Briegel, H.J., *Phys. Rev. Lett.* **2005**, 95, 120405.
- [35] Cabello, A., *Phys. Rev. Lett.* **2001**, 87, 010403.
- [36] Einstein, A.; Podolsky, B.; Rosen, N., *Phys. Rev.* **1935**, 47, 777.

Appendix: Comparison of Local Realism Violation

Here, we compare the violation degrees to the Bell inequality of the GHZ-type states:

$$|\psi_1\rangle = (|H_1H_2\cdots H_m\rangle + |V_1V_2\cdots V_m\rangle)^{\otimes 3},$$

$$|\psi_2\rangle = (|H_1H_2\cdots H_n\rangle + |V_1V_2\cdots V_n\rangle)^{\otimes 2},$$

$$|\psi_3\rangle = (|H_1H_2\cdots H_l\rangle + |V_1V_2\cdots V_l\rangle),$$

where the superscripts 3, 2, 1 represent the number of entangled DOFs; m, n, l signify the photon numbers, and satisfy $m \times 3 = n \times 2 = l \times 1$, i.e they have the same qubits. According to the method in calculating the state (1) in the text, we just need to calculate the number of S_i with negative sign, labeled as $C(\psi)$. The larger $C(\psi)$ means a bigger violation.

First, we compute the $C(\psi)$ of the state which has m photons in one DOF by taking the advantage of equation:

$$C(\psi) = C_m^2 + C_m^6 + \dots + C_m^{2+4i} \quad (A1)$$

with $2i + 4 \leq m$. For different values of m , the above equation tells

$$C(\psi) = \begin{cases} 2^{m-2} & \text{if } m = 4x - 2 \\ (-1)^{\frac{m+5}{4}} 2^{\frac{m-3}{2}} + 2^{m-2} & \text{if } m = 4x - 1 \\ (-1)^{\frac{m+4}{4}} 2^{\frac{m-2}{2}} + 2^{m-2} & \text{if } m = 4x \\ (-1)^{\frac{m+3}{4}} 2^{\frac{m-3}{2}} + 2^{m-2} & \text{if } m = 4x + 1 \end{cases}, \quad (A2)$$

where $x = 1, 2, \dots$.

Then, we arrive at the results in following ten different cases:

1. m is odd and $m = 4x - 1$. In this case $n = \frac{3m}{2}$ is not integer, $l = 3m = 12x - 3$, so

$$C(\psi_1) - C(\psi_3) = 3((-1)^{\frac{x+1}{4}} 2^{2x-2} + 2^{4x-3})(2^{4x-1} - (-1)^{\frac{x+1}{4}} 2^{2x-2} - 2^{4x-3})^2 + ((-1)^{\frac{x+1}{4}} 2^{2x-2} + 2^{4x-3})^3 - ((-1)^{3x} 2^{6x-3} + 2^{12x-5}) = -3 \times 2^{-7+6x} \times (8 \times (-1)^x + (-1)^x \times 2^{1+4x} + 4^{1+x} - 64^x) > 0, \text{ for } x = 1, 2, \dots$$

2. m is odd and $m = 4x + 1$. In this case $n = \frac{3m}{2}$ is not integer, $l = 3m = 12x + 3$, so

$$C(\psi_1) - C(\psi_3) = 3((-1)^{\frac{x+1}{4}}2^{2x-1} + 2^{4x-1})(2^{4x+1} - (-1)^{\frac{x+1}{4}}2^{2x-1} - 2^{4x-1})^2 + ((-1)^{\frac{x+1}{4}}2^{2x-1} + 2^{4x-1})^3 - ((-1)^{3x+2}2^{6x} + 2^{12x+1}) = -3 \times 2^{-1+6x} \times ((-16)^x + (-1)^x + 4^x - 64^x) > 0 \text{ for } x = 1, 2, \dots$$

3. m is even and $m = 8x + 2$. In this case $n = \frac{3m}{2} = 12x + 3$, so

$$C(\psi_1) - C(\psi_2) = 3(2^{8x})(2^{8x+2} - 2^{8x})^2 + (2^{8x})^3 - 2((-1)^{3x+2}2^{6x} + 2^{12x+1})(2^{12x+3} - (-1)^{3x+2}2^{6x} - 2^{12x+1}) = 2^{1+12x} + 4^{1+12x} - (-1)^x \times 8^{1+6x} > 0 \text{ for } x = 0, 1, \dots$$

4. m is even and $m = 8x - 2$. In this case $n = \frac{3m}{2} = 12x - 3$, so

$$C(\psi_1) - C(\psi_2) = 3(2^{8x-4})(2^{8x-2} - 2^{8x-4})^2 + (2^{8x-4})^3 - 2((-1)^{3x}2^{6x-3} + 2^{12x-5})(2^{12x-3} - (-1)^{3x}2^{6x-3} - 2^{12x-5}) = 4^{-5+6x} \times (32 + 4^{6x} - (-1)^x 4^{2+3x}) > 0 \text{ for } x = 1, 2, \dots$$

5. m is even and $m = 8x + 4$. In this case $n = \frac{3m}{2} = 12x + 6$, so

$$C(\psi_1) - C(\psi_2) = 3((-1)^{2x+2}2^{4x+1} + 2^{8x+2})(2^{8x+4} - (-1)^{2x+2}2^{4x+1} - 2^{8x+2})^2 + ((-1)^{2x+2}2^{4x+1} + 2^{8x+2})^3 - 2(2^{12x+4})(2^{12x+6} - 2^{12x+4}) = 2^{5+12x} \times (1 - 3 \times 2^{1+4x} + 3 \times 4^{1+4x} + 8^{1+4x}) > 0 \text{ for } x = 0, 1, \dots$$

6. m is even and $m = 8x$. In this case $n = \frac{3m}{2} = 12x$, so

$$C(\psi_1) - C(\psi_2) = 3((-1)^{2x+1}2^{4x-1} + 2^{8x-2})(2^{8x} - (-1)^{2x+1}2^{4x-1} - 2^{8x-2})^2 + ((-1)^{2x+1}2^{4x-1} + 2^{8x-2})^3 - 2((-1)^{3x+1}2^{6x-1} + 2^{12x-2})(2^{12x} - (-1)^{3x+1}2^{6x-1} - 2^{12x-2}) = 16^{-1+4x} \times (-12 + (-1)^x \times 2^{3+2x} - 3 \times 2^{1+4x} + 256^x) > 0 \text{ for } x = 1, 2, \dots$$

7. n is even and $n = 4x - 2$. In this case $l = 2n = 8x - 4$, so

$$C(\psi_2) - C(\psi_3) = 2(2^{4x-4})(2^{4x-2} - 2^{4x-4} - ((-1)^{2x}2^{4x-3} + 2^{8x-6})) = 2^{-7+4x} \times (-16 + 16^x) > 0 \text{ for } x = 2, 3, \dots$$

8. n is even and $n = 4x$. In this case $l = 2n = 8x$, so

$$C(\psi_2) - C(\psi_3) = 2((-1)^{x+1}2^{2x-1} + 2^{4x-2})(2^{4x} - (-1)^{x+1}2^{2x-1} - 2^{4x-2}) - ((-1)^{2x+1}2^{4x-1} + 2^{8x-2}) = 8^{-1+2x} \times (-4 \times (-1)^x + 4^x) > 0 \text{ for } x = 1, 2, \dots$$

9. n is odd and $n = 4x - 1$. In this case $l = 2n = 8x - 2$, so

$$C(\psi_2) - C(\psi_3) = 2((-1)^{x+1}2^{2x-2} + 2^{4x-3})(2^{4x-1} - (-1)^{x+1}2^{2x-2} - 2^{4x-3}) - (2^{8x-4}) = 2^{-5+4x} \times (-4 - (-1)^x \times 4^{1+x} + 16^x) > 0 \text{ for } x = 1, 2, \dots$$

10. n is odd and $n = 4x + 1$. In this case $l = 2n = 8x + 2$, so

$$C(\psi_2) - C(\psi_3) = 2((-1)^{x+1}2^{2x-1} + 2^{4x-1})(2^{4x+11} - (-1)^{x+1}2^{2x-1} - 2^{4x-1}) - (2^{8x}) = 2^{-1+4x} \times (-1 - (-1)^x \times 2^{1+2x} + 16^x) > 0 \text{ for } x = 1, 2, \dots$$

In conclusion, it is evident that $C(\psi_1) > C(\psi_2) > C(\psi_3)$, which tells that for the three GHZ-type entangled states with same qubits, the one entangled in three DOFs, the ψ_1 , violates LR most, the state ψ_2 entangled in two DOFs violates the second, and the state ψ_3 entangled only in one DOF violates the least.

Table 1: Comparison of violation degree for different entangled states.

state	$\langle B \rangle_{QM}$	$max_{LHVT} \langle B \rangle $	$D = \langle B \rangle_{QM} / max_{LHVT} \langle B \rangle $
ψ	4096	388	10.56
ψ'	4096	1024	4.00
ψ''	4096	1984	2.06

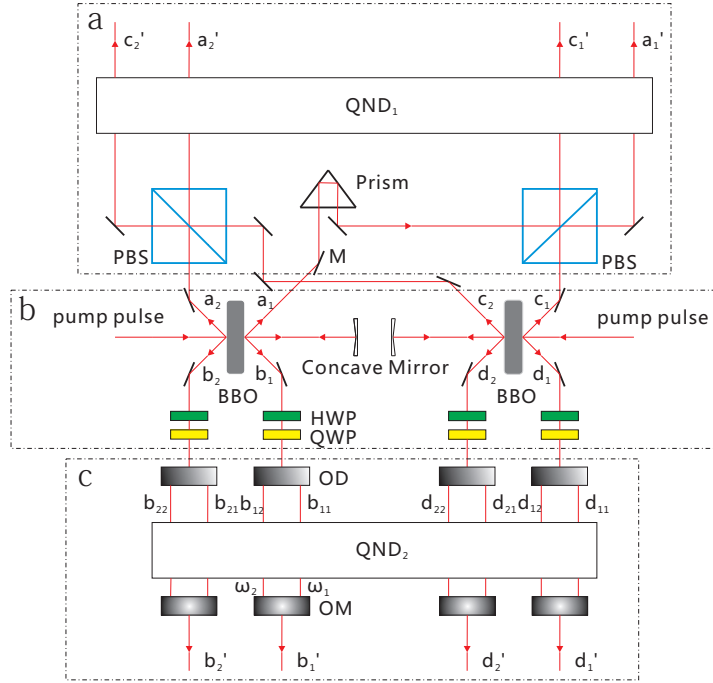


Figure 1: Preparation scheme. a) SPDC source. The two sets of crystal system generate photon pairs entangled in polarization, frequency and spatial mode respectively. b) Design of constructing the entanglement of four photons with one another in polarization and spatial mode. Two PBSs are exploited to implement the selection of polarization, and a cross-kerr nonlinear medium which can accomplish the function as quantum nondemolition detector (QND) is used to choose photons' spatial modes. c) Design of constructing the entanglement of four photons with one another in frequency and spatial mode. Analogously, the selection of frequency is achieved by four sets of Wavelength Division Multiplexer (WDM) which consists of optical demultiplexer (OD) and optical multiplexer (OM). Moreover, the complete experimental set still needs one more cross-kerr nonlinear medium to choose photons' spatial modes the same as explained in above.

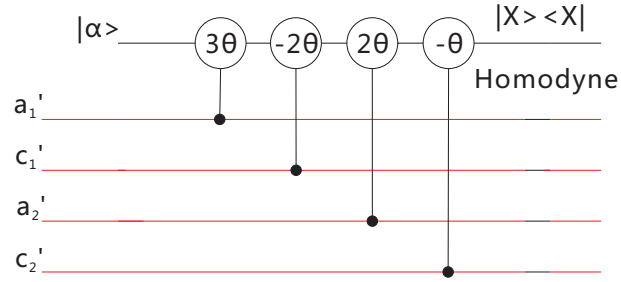


Figure 2: QND_1 . The realization of selecting paths of photons a and c with cross-kerr nonlinear medium.

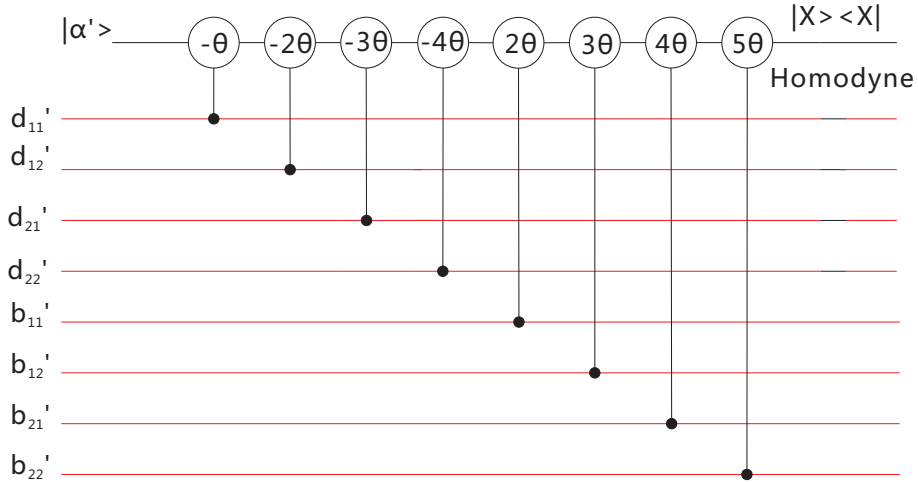


Figure 3: QND_2 . The realization of selecting paths of photons b and d with cross-kerr nonlinear medium.

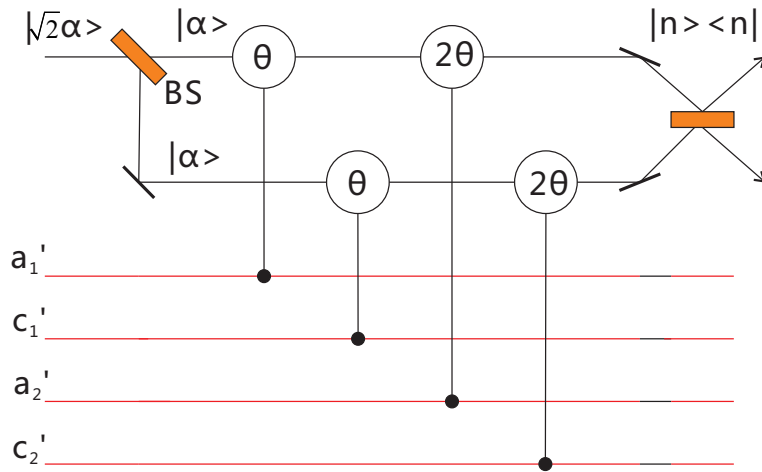


Figure 4: Double XPM method to realize the function of Fig. 2.

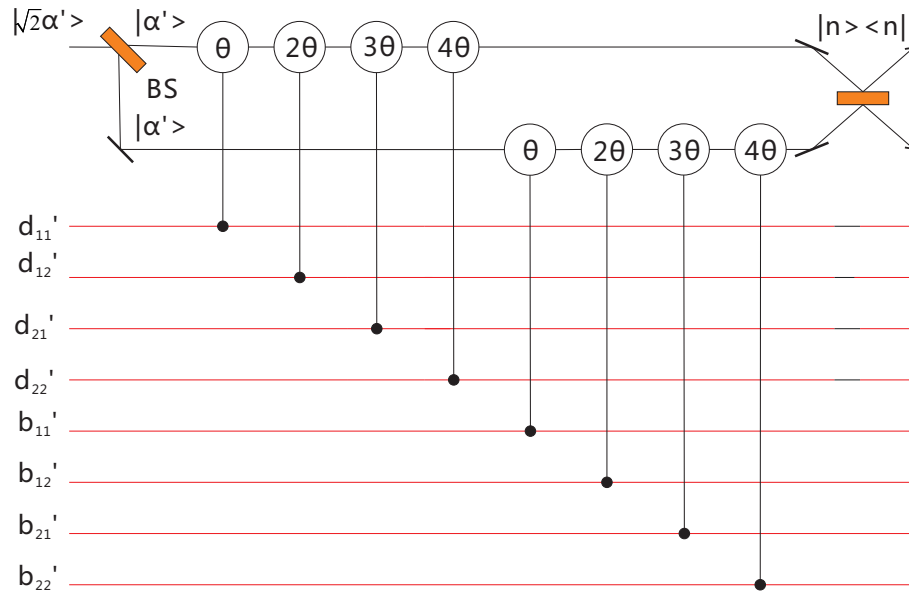


Figure 5: Double XPM method to realize the function of Fig. 3.

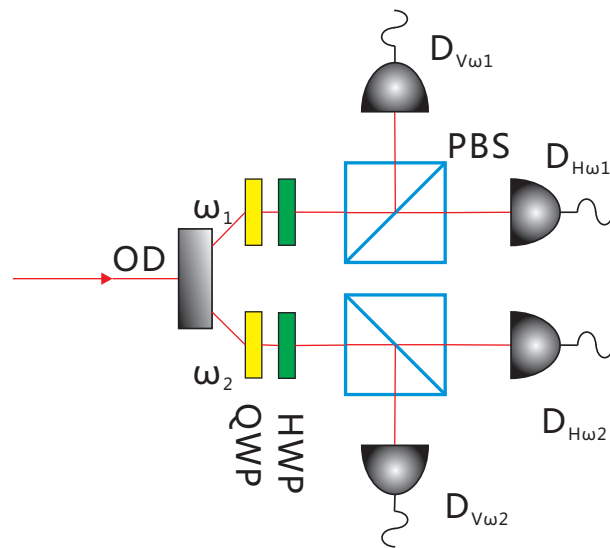


Figure 6: Measurement setup. OD: optical demultiplexer; QWP: quarter-wave plate; HWP: half-wave plate; PBS: polarizing beam splitter; D: single-photon detector.